Geol. Mag. **135** (*1*), *1997, pp. 15–26. Printed in the United Kingdom*

The Lower Silurian Osmundsberg K-bentonite. Part II: mineralogy, geochemistry, chemostratigraphy and tectonomagmatic significance

WARREN D. HUFF*, STIG M. BERGSTRÖM†, DENNIS R. KOLATA‡ & HEPING SUN*

* Department of Geology, University of Cincinnati, Cincinnati, OH 45221-0013, USA; warren.huff@uc.edu; sunhp@ucunix.san.uc.edu
† Department of Geological Sciences, The Ohio State University, 155 S. Oval Mall, Columbus, OH 43210, USA; stig@geology. ohio-state.edu
‡ Illinois State Geological Survey, 615 E. Peabody Dr., Champaign, IL 61820, USA; kolata@geoserv.isgs.uiuc.edu

(*Received* 28 January 1997; *accepted* 14 August 1997)

Abstract – The Lower Silurian Osmundsberg K-bentonite is a widespread ash bed that occurs throughout Baltoscandia and parts of northern Europe. This paper describes its characteristics at its type locality in the Province of Dalarna, Sweden. It contains mineralogical and chemical characteristics that permit its regional correlation in sections elsewhere in Sweden as well as Norway, Estonia, Denmark and Great Britain. The < 2 μm clay fraction of the Osmundsberg bed contains abundant kaolinite in addition to randomly ordered (RO) illite/smectite (I/S). Modelling of the X-ray diffraction tracings showed the I/S consists of 18 % illite and 82 % smectite. The high smectite and kaolinite content is indicative of a history with minimal burial temperatures. Analytical data from both pristine melt inclusions in primary quartz grains as well as whole rock samples can be used to constrain both the parental magma composition and the probable tectonic setting of the source volcanoes. The parental ash was dacitic to rhyolitic in composition and originated in a tectonically active collision margin setting.

Whole rock chemical fingerprinting of coeval beds elsewhere in Baltoscandia produced a pronounced clustering of these samples in the Osmundsberg field of the discriminant analysis diagram. This, together with well-constrained biostratigraphic and lithostratigraphic data, provides the basis for regional correlation and supports the conclusion that the Osmundsberg K-bentonite is one of the most extensive fallout ash beds in the early Phanerozoic. The source volcano probably lay to the west of Baltica as part of the subduction complex associated with the closure of Iapetus.

1. Introduction

The Lower Silurian (Llandoverian) Kallholn Shale of central Sweden contains a well-preserved sequence of K-bentonite beds, the most prominent of which is the Osmundsberg K-bentonite bed (Bergström *et al.* 1993). The type section of the Osmundsberg is in an abandoned quarry in the eastern part of the Siljan impact structure in the Province of Dalarna (Fig. 1) where the Kallholn Shale unconformably overlies the Upper Ordovician Boda Limestone (Fig. 2). The Osmundsberg bed is 1.15 m thick at this locality and is accompanied in approximately 10 m of section by eight additional K-bentonite beds which range between 1 and 32 cm in thickness. The succession lies within the *sedgwickii* and *turriculatus* graptolite zones, and the *D. kentuckyensis* and *D. staurognathoides* conodont zones (Bergström *et al.* 1998, this issue) The abundance and thickness of this succession together with the similarity of biostratigraphically coeval ash beds elsewhere constitutes the basis for a study of the geographic extent and the stratigraphic and palaeotectonic significance of these beds. Samples were collected from exposures and cores which include the *turriculatus* Zone elsewhere in Sweden as well as Norway, Denmark, Great Britain and Estonia. Chemostratigraphic and biostratigraphic data were used to evaluate the regional distribution pattern. We conclude from this study that the Osmundsberg K-bentonite is present in all of these localities and that it represents a subduction-related, explosively erupted felsic ash with a magnitude and character similar to some of the thickest and most widespread Ordovician ash beds (Kolata, Frost & Huff, 1987; Huff & Kolata, 1990; Huff *et al.* 1996). This paper reports the mineralogical and geochemical characteristics of the Osmundsberg bed that form part of the basis for this conclusion.

2. Mineralogy

The Osmundsberg and associated beds consist largely of clay minerals accompanied by a variety of primary volcanogenic crystals and secondary sulfides, sulfates, oxides, carbonates and silicates. Although the clay mineral composition of Lower Palaeozoic K-bentonites is generally distinctive compared with adjacent siliciclastic rocks, their volcanic origin can be confirmed through the recognition of fragmented or euhedral phenocrysts[1] of

[1] Phenocryst is here used to describe juvenile crystal pyroclasts which are products of parental magma crystallization and have been emplaced as discrete fallout particles (see Huff *et al*. 1996).

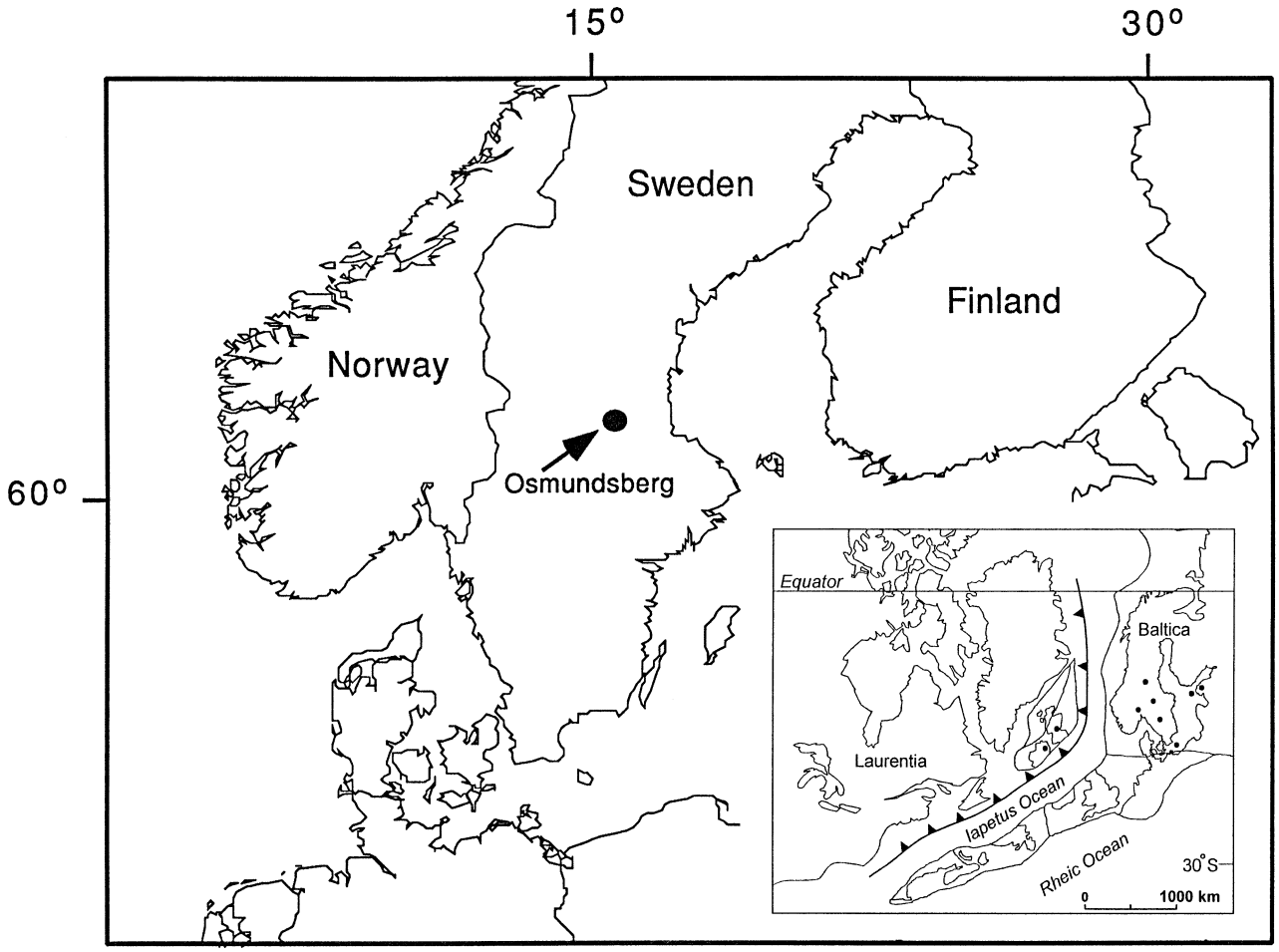

Figure 1. The type section of the Osmundsberg K-bentonite occurs in south-central Sweden (Dalarna) near the margin of the Siljan Ring impact structure. The inset map shows the inferred position of Laurentia, Avalonia and Baltica during early Silurian closure of the Iapetus ocean as interpreted by McKerrow *et al.* (1991). Note the presence of an active subduction zone on the western margin of Iapetus, which may have included the volcano(es) responsible for the Osmundsberg K-bentonite.

volcanic origin. Mineral isolation in K-bentonites was accomplished by wet sieving of the bulk sample followed by magnetic and heavy liquid separation treatments. Samples were wet sieved to isolate coarse mineral grains which were then separated by further sieving into two fractions, 75–250 μm and > 250 μm. Mineral identification was made using petrographic and stereo-zoom microscopic methods, and additionally by using powder X-ray diffraction and energy-dispersive analysis on the scanning electron microscope. Grain counts of the mineral grains in the 75–250 μm fraction were made under a stereo-zoom microscope. For each sample, about 300 grains were counted for calculating the percentages of major minerals. The dominant non-clay mineral composition of the coarse fraction consisted of biotite, quartz and sanidine with lesser amounts of apatite, zircon and anatase. Other than clay minerals, calcite and pyrite are the most common secondary minerals present.

2.a. Quartz

Most of the quartz grains in the Osmundsberg are broken, subangular to splintery, monocrystalline and water-clear to slightly cloudy. The majority of particles vary in maximum dimension between 100 and 300 μm. There are up to a few per cent of beta-form quartz paramorph crystals commonly having subhedral crystal faces and edges. A few of these grains are embayed and show evidence of slight dissolution. Glass melt inclusions occur commonly in the paramorphs (Fig. 3a) and have been analysed by electron microprobe to determine parental magma composition at the time of quartz crystallization.

2.b. Biotite

Biotite accounts for 11–41 % of the phenocryst grains in the studied samples. Individual flakes range from dark brown to nearly colourless (Fig. 3b) depending upon their degree of alteration. Abundant highly altered biotite flakes occur mainly in the basal portion of the Osmundsberg K-bentonite. They appear in various colours under the polarizing microscope and were separated magnetically into three fractions: paramagnetic (strongly magnetic), intermediate and diamagnetic (weakly magnetic). Most flakes in the paramagnetic fraction are dark brown, those in the intermediate fraction are brownish yellow, and those in the diamagnetic fraction are colourless and highly transparent.

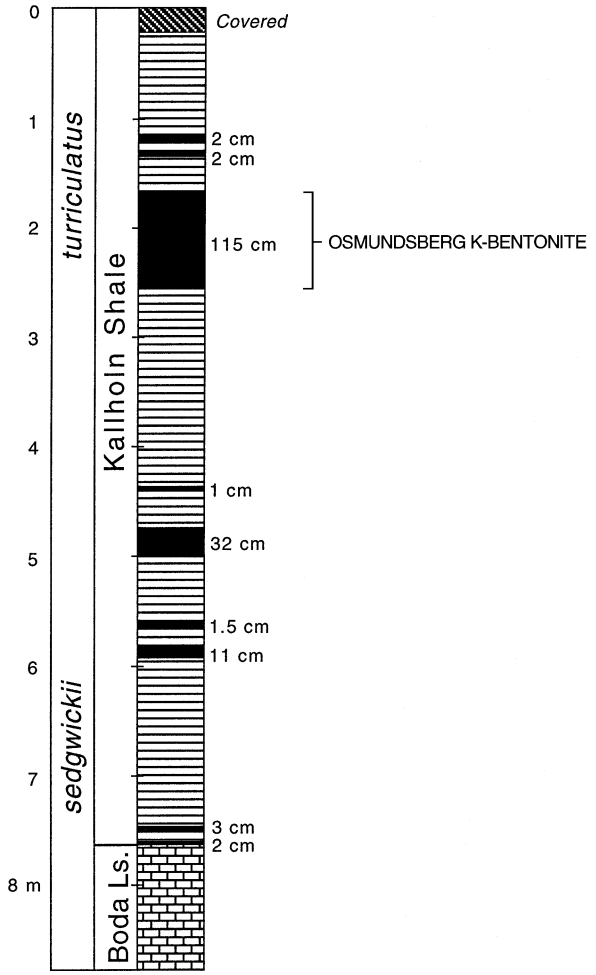

Figure 2. Stratigraphic position of the Osmundsberg K-bentonite at its type section in Dalarna. The Kallholn Shale at this locality contains nine K-bentonite beds (solid black bands) ranging from 1–115 cm in thickness. The section lies unconformably on the Boda Limestone, and both units fall within the *turriculatus* graptolite zone.

XRD patterns from oriented specimens of three altered biotite fractions show three phases: kaolinite (7 Å), biotite (10 Å) and chlorite/smectite (14.5 Å) (Fig. 4). The content of chlorite/smectite decreases from paramagnetic, intermediate, to diamagnetic fractions. The diamagnetic fraction is purely kaolinite in composition as shown by qualitative energy dispersive X-ray spectra. On XRD patterns of ethylene glycol solvated specimen, the 14.5 Å peak divides into two peaks at 15.76 Å and 13.6 Å (Fig. 5). This is characteristic of mixed-layer clays in which one component is a swelling phase and the other is non-swelling (Moore & Reynolds, 1989). The peak collapses to a small 14.04 Å peak after heating to 375 °C, and a superlattice peak which was not detected in the initial diffraction tracings appeared at 19.68 Å. Using the computer program NEWMOD (Reynolds, 1985), the 15.76 Å and 13.62 Å peaks on the ethylene glycol XRD pattern were interpreted as R1 or short-range ordered mixed-layer smectite/chlorite with approximately equal proportions of each component.

Back-scattered electron images show that altered biotite flakes from the paramagnetic fraction consist of lamellae with bright and dark contrasts (Fig. 6). Energy-dispersive X-ray spectra from bright lamellae have peaks of Si, Al, K, Fe, Mg and Ti, typical of biotite-chlorite compositions. Those from dark lamellae have only two peaks of Si and Al in a ratio of about 1 : 1, indicating a pure kaolinite composition, commonly a characteristic of authigenic kaolinite.

On the basis of the above data, we suggest that the altered biotite flakes in the Osmundsberg K-bentonite consist of alternating kaolinite and chloritized biotite lamellae. The alteration of biotite flakes involves two processes: (1) biotite transforming to chlorite and smectite through loss of potassium, and (2) neoformation of kaolinite crystallites by epitaxial growth on the layer silicate surfaces. Biotite transforming to chlorite and smectite is accomplished by lateral layer replacement and layer modification (Banfield & Eggleton, 1988; Jiang & Peacor, 1994), whereas new kaolinite crystallites form and expand in biotite cleavage space. Close examination of the back-scattered SEM image in Figure 6 shows each kaolinite region characterized by a seam which bisects the crystal growth region. This line represents the termination of kaolinite crystal growth which was initiated on the mica surface. This interpretation is supported by the splintered appearance of residual mica cleavage fragments which results from the expansion pressure of kaolinite growth.

2.c. Zircon

Zircons occur as colourless, pale pink and sometimes yellowish red euhedral prismatic crystals (Fig. 3c). Crystals are small with lengths of 70–180 µm. The length-to-width (aspect) ratios are about 1.9 : 1 to 2.7 : 1. The quantity compared with other primary minerals is very small, ranging from tens to perhaps hundreds of grains in 500 g of sample. The crystals usually have sharp faces and edges and many show complex patterns of zoning. Rounded cores are evident in some crystals, suggesting inheritance of older zircon from pre-existing basement rocks with precipitation of additional zircon by the Osmundsberg magma. Some of them are broken and most contain glass and mineral inclusions.

2.d. Apatite

Apatites occur as milky white and yellowish white euhedral prismatic crystals. Most of them have etched surfaces (Fig. 3d). It is a minor mineral in the amount of a few hundred milligrams in 500 g of sample. They are slightly larger than the zircon crystals, with lengths of 80–220 µm. The aspect ratios are about 1.3 : 1 to 3.2 : 1. Small glass inclusions are also seen in the apatite crystals.

2.e. Sanidine

Primary sanidine occurs as clear to slightly cloudy, glassy and sharply outlined grains. It is difficult to distinguish it

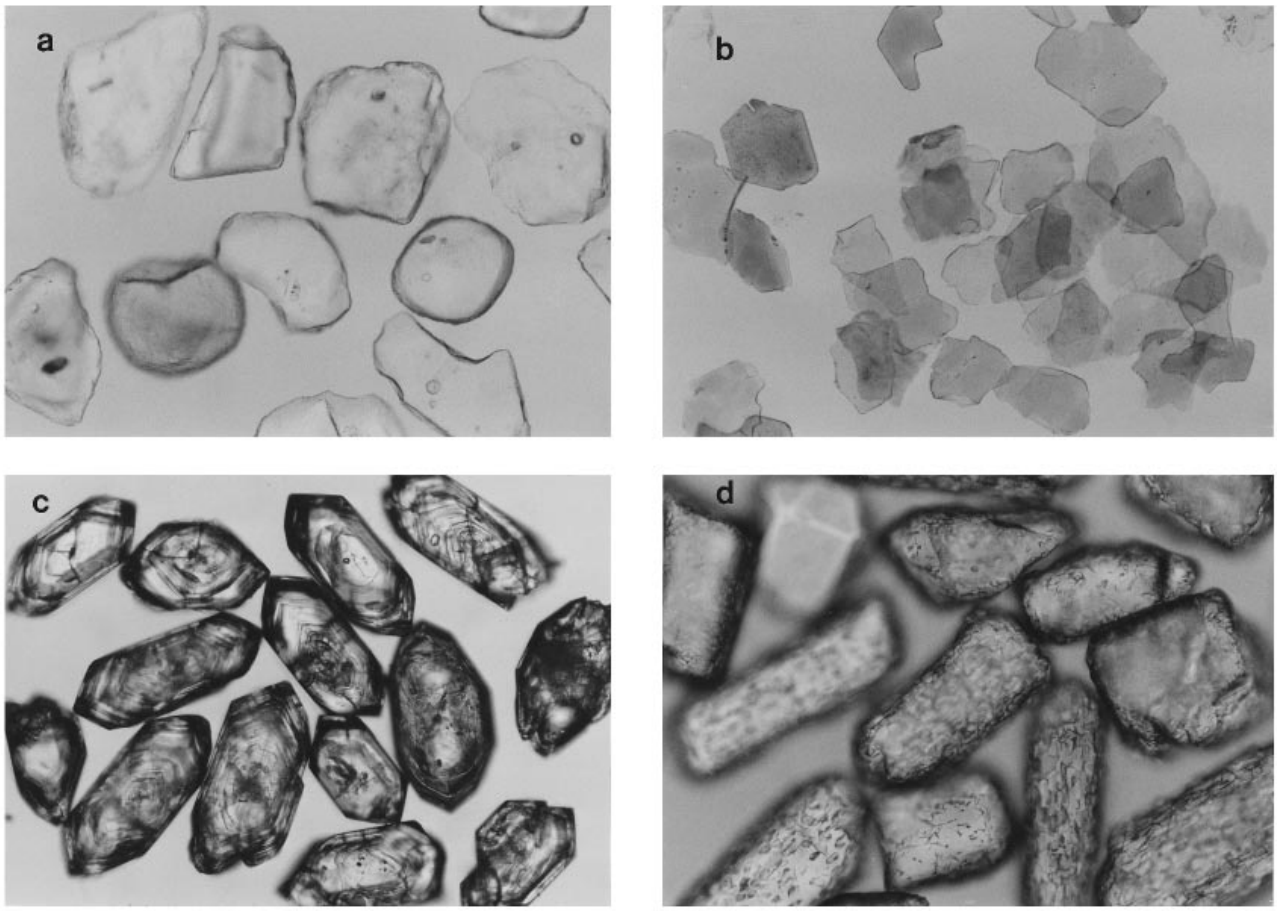

Figure 3. Examples of volcanogenic phenocrysts from the Osmundsberg K-bentonite bed. (a) Beta-form, etched and resorbed, subrounded quartz grains. Many contain inclusions of pristine glass representing melt composition at the time of quartz crystallization; (b) biotite flakes; (c) euhedral and zoned zircon crystals; and (d) euhedral and etched apatite crystals. The width of the field of view of (a) and (b) is 1.04 mm, and that of (c) and (d) is 0.52 mm.

from quartz under the petrographic microscope, but because sanidine has lower relief than quartz, it is easy to distinguish grains with polished surfaces under reflected light. The presence of sanidine is also confirmed by X-ray diffraction and energy-dispersive analysis of X-rays. The EDS spectra qualitatively show the major elemental composition of Si, K and Al with small amounts of Ca and Na.

2.f. Anatase

Anatase appears as occasional orange-brown skeletal grains 100-200 μm in diameter which were separated together with apatite and zircon crystals by heavy liquid methods. Identification was confirmed by a well-defined peak at 3.51 Å and subsequent peaks at higher angles (Fig. 7).

3. Clay mineralogy

Clay minerals derived from the alteration of felsic volcanic ash are sensitive to the thermal conditions and geochemical environments which have characterized their post-emplacement history. In contrast to the clay minerals in Mesozoic and Cenozoic bentonites, which are generally dominated by smectite, Palaeozoic K-bentonite are typified by mixed-layer illite/smectite (I/S) assemblages with illite as the dominant phase. They are frequently accompanied by lesser amounts of kaolinite, discrete illite and mixed-layer chlorite/smectite (C/S). Previous studies have concluded that I/S in K-bentonites as well as shales is a diagenetic product of smectite alteration (Altaner *et al.* 1984; Bethke, Vergo & Altaner, 1986; Brusewitz, 1988; Anwiller, 1993) and that further alteration to C/S occurs under low grade metamorphic conditions (Krekeler & Huff, 1993).

The < 2 μm clay fractions of the top, middle and bottom of the Osmundsberg bed from the type locality were separated by the suspension method and were prepared as oriented specimens on glass petrographic slides. The clay mineral composition was determined by powder X-ray diffraction analysis of the glycol-saturated specimens, and the data are shown in Figure 8. Silurian K-bentonites frequently contain more kaolinite in addition to I/S compared with Ordovician beds as shown, for example, by occurrences in Great Britain (Huff, Morgan & Rundle, 1997). Current studies (Huff, 1997) indicate this reflects primarily a facies influence and especially the availability of potassium during diagenesis and is not simply a response to thermal history.

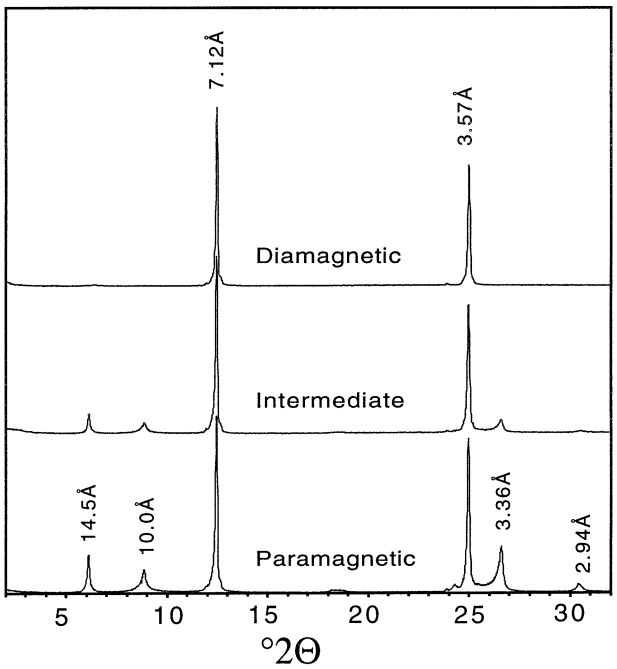

Figure 4. Powder X-ray diffraction (XRD) patterns of paramagnetic (strongly magnetic), intermediate and diamagnetic (weakly magnetic) biotite flakes. Phases include kaolinite (7.12 Å/3.57 Å), biotite (10.01 Å) and chlorite–smectite (14.5 Å).

The Osmundsberg and associated K-bentonites are marked by a single prominent peak at 16.9 Å on the glycolated pattern which we interpret as representing randomly interstratified (R0) I/S. Modelling of the diffraction tracings using NEWMOD (Reynolds, 1985) showed the samples contain 18 % illite and 82 % smectite. The same conclusion results from consideration of the $\Delta 2\Theta$ value of 5.64, which measures the difference between the 001/002 and 002/003 reflections of I/S (Moore & Reynolds, 1989). Kaolinite is represented by prominent reflections at 7.15 Å and 3.57 Å. It is interesting to note that while kaolinite is a common accessory clay mineral in Silurian K-bentonites, the R0 form of I/S is unusual. For example, Huff, Morgan & Rundle (1997) report Llandovery through Ludlow K-bentonites in Great Britain typically contain R1 ordered I/S plus varying amounts of kaolinite, and Huff *et al.* (1991) reported long-range or R3 ordered I/S in Llandovery K-bentonites from northern Ireland and the Southern Uplands of Scotland. Batchelor & Weir (1988) interpreted powder diffraction analysis of K-bentonite clays from the Southern Uplands as R0 I/S, but their XRD tracings clearly show R3 ordering. Silurian K-bentonites from Podolia, Ukraine, contain R0 ordered I/S in carbonate facies and R1–R3 ordered I/S in the shale facies (Huff, 1997). The preservation of randomly ordered I/S is normally interpreted as indicative of a shallow burial history with relatively low temperatures, with a transition to ordered forms during increased burial. While this may be true for shales and mudrocks during basinal subsidence, the Podolian sequence of K-bentonites, which occurs on the edge of the Russian platform and has no history of deep burial, clearly suggests that facies and K-availability factors play a leading role in determining clay mineral characteristics.

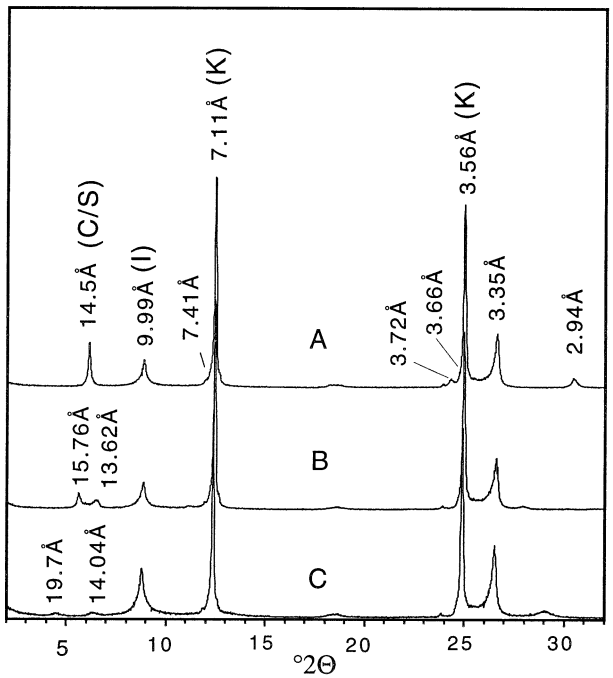

Figure 5. Powder X-ray diffraction patterns of interstratified chlorite–smectite analysed as (A) air-dried, (B) ethylene glycol saturated and (C) heated (375 °C) oriented slides. The splitting of the 14.5 Å air-dried peak following glycolation reveals the mixed-layer character of the sample.

4. Geochemistry

Geochemical data can be applied both to the interpretation of the tectonomagmatic setting of the source volcanoes and to the chemostratigraphic correlation of the individual layers. Whole-rock major and trace element analyses of the Osmundsberg ash bed (Table 1) were conducted on dried and powdered samples. The major-oxide compositions were established by X-ray fluorescence (XRF), and trace and rare elarth elements by instrumental neutron activation analysis (INAA) and ICP analysis. The chemical composition of glass melt inclusions in quartz crystals was determined by electron microprobe (Table 2).

Immobile trace elements and rare earth elements (REE) have been used by numerous workers to provide information on the magmatic composition of K-bentonite parent ashes and tectonic setting of the source volcanoes (Teale & Spears, 1986; Huff, Morgan & Rundle, 1997; Merriman & Roberts, 1990). These studies have generally relied on the use of empirically based discrimination plots derived from studies of igneous rocks of known origin, and while not providing absolute proof of magmatic origin or affinity, these diagrams serve as useful sources of information about the tectonic settings and general magma chemistries, particularly in cases where other geological evidence is ambiguous. For K-bentonites which are the

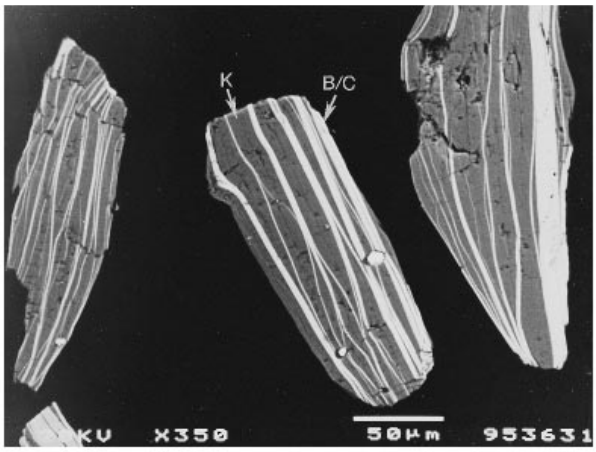

Figure 6. Back-scattered electron image of three altered biotite flakes from the paramagnetic portion. Lamellae with bright contrast are biotite–chlorite and those with dark gray contrast are kaolinite.

altered remains of pyroclastic deposits we rely principally on immobile trace elements for information about original magma chemistry. Previous studies have shown that those elements which tend to be unaffected by weathering or that reside in as yet unaltered primary phenocrysts are reliable indicators of past rock history (Teale & Spears, 1986; Huff, Morgan & Rundle, 1997; Merriman & Roberts, 1990). TiO_2, the high field strength (HFS) elements Zr, Nb, Hf, Ta and the rare earth elements (REE) are commonly considered to be immobile under most conditions of diagenesis and low grade metamorphism, and are thus useful indicators of petrogenetic processes. The Nb/Y ratio is widely used as a measure of alkalinity and Zr/TiO_2 as an index of differentiation. Many explosively erupted volcanic ashes tend to have moderate to high Nb and Zr content reflective of their silicic and high volatile (H_2O) character (Izett, 1981). A plot of Zr/TiO_2 against Nb/Y (Fig. 9) after Winchester & Floyd (1977) shows that most Osmundsberg K-bentonites are subalkaline to alkaline in nature and derived from silicic magmas which were trachyandesite to dacite in composition. As shown in Table 2, the composition of glass melt inclusions are rhyolitic, and

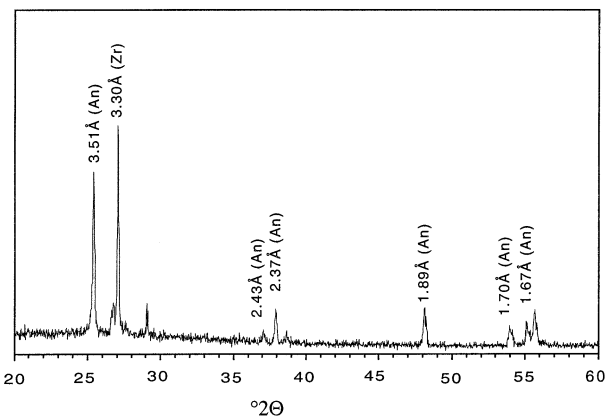

Figure 7. Powder X-ray diffraction pattern of anatase (An) and zircon (Zr) in the heavy mineral fraction of the Osmundsberg K-bentonite.

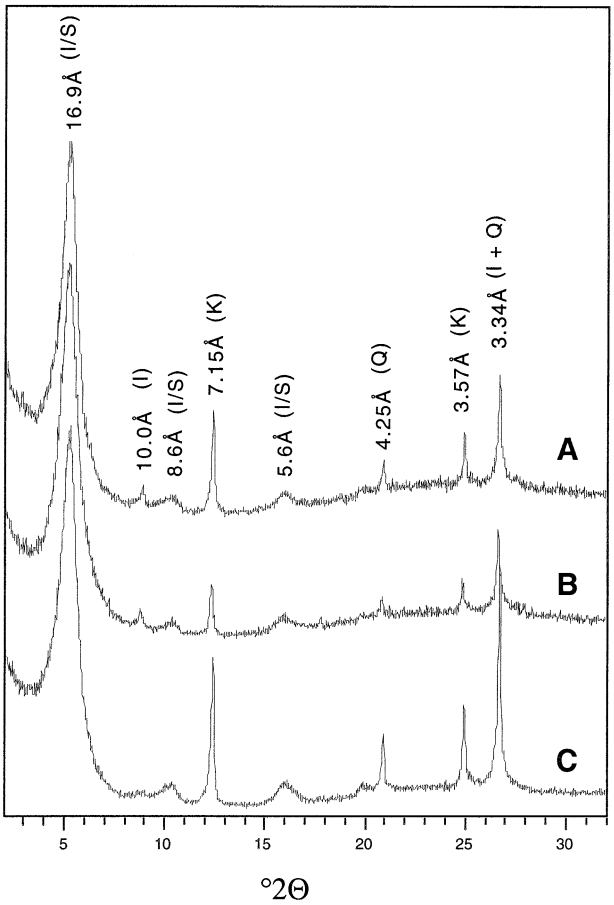

Figure 8. Powder X-ray diffraction patterns of the <2 µm oriented, glycol-saturated specimens from the top (A), middle (B) and bottom (C) of the Osmundsberg K-bentonite. Computer modelling reveals the dominant phase is a randomly ordered (R0) illite/smectite with lesser amounts of kaolinite and a trace of quartz.

if they are truly indicative of the pre-eruptive magma type then Y must be slightly mobile during the formation of K-bentonite. The water content of the Osmundsberg K-bentonite is approximately 5 % by weight based on the volatile content of glass melt inclusions, and it is the explosive release of this volatile component that initiates the transport of ash and pumice fragments over thousands of square kilometres, producing the K-bentonite stratigraphic record. The silicic nature further implies that the parent magmas are not wholly mantle-derived but contain a significant portion of continental crustal material. Table 2 lists the major oxide values for 14 pristine melt inclusions from the type Osmundsberg bed. The mean anhydrous SiO_2 content of glass inclusions is 77.7 %. Data points on an alkali ternary diagram (Fig. 10) for glass inclusions plot in a narrow region close to the alkali join (K_2O–Na_2O). When compared with average acidic volcanic rocks (Nockolds, 1954) the molar ratio of $(K_2O + Na_2O + CaO)/Al_2O_3$ is 0.90 for glass inclusions, which indicates that the pre-eruptive magma was a high-silica calc-alkaline and alkaline rhyolite with peraluminous affinities. Quartz crystallization trapped liquid that reflects this composition.

Table 1. Major and trace element analyses of the Osmundsberg K-bentonite

Sample	NOR30	SWE92	SWE96A	SWE128	SWE129	SWE131	SWE132	SWE137	EST-131	WDH-47	DEN8
SiO_2	47.80	59.10	63.10	51.00	58.30	61.30	54.20	61.30	61.70	58.00	22.60
Al_2O_3	18.90	16.70	17.00	15.60	19.40	17.10	18.30	16.70	18.00	23.80	12.60
Fe_2O_3	3.26	4.06	3.09	7.18	2.40	2.36	2.44	5.13	1.26	2.53	31.80
MgO	3.61	3.49	3.21	2.43	2.70	3.23	2.74	2.55	1.22	1.26	0.97
CaO	8.72	2.76	1.81	3.49	3.72	3.32	6.80	0.58	0.23	0.71	1.98
Na_2O	0.38	2.33	1.16	0.01	0.11	0.07	0.08	0.57	0.10	0.63	0.10
K_2O	6.45	4.05	4.69	3.30	1.60	1.32	1.69	3.97	14.10	4.25	3.00
TiO_2	0.47	0.88	0.32	0.87	0.58	0.41	0.56	0.84	0.37	0.78	0.97
P_2O_5	0.17	0.32	0.13	0.07	0.29	0.14	0.26	0.07	0.18	0.08	0.17
MnO	0.06	0.04	0.03	0.03	0.06	0.04	0.09	0.16	0.02	0.03	0.09
LOI	9.35	5.65	4.90	14.30	10.80	10.80	12.00	7.70	1.85	8.08	26.20
Total	99.36	99.51	99.55	98.39	100.1	100.2	99.32	99.72	99.15	100.3	100.6
Nb	18	14	14	13	14	12	12	10	14	40	12
V	45	85	21	110	47	34	48	110	25	14	78
Dy	6.7	2.5	2.4	3.0	2.0	1.5	2.5	11.0	0.9	14.4	17.4
Ho	1.07	0.33	0.35	0.63	0.37	0.27	0.45	1.85	0.13		3.34
Er	11.0	1.0	1.1	2.0	1.1	0.7	1.1	5.1	0.4		9.2
Tm	0.3	0.1	0.1	0.3	0.1	0.1	0.1	0.7	0.1		1.3
Yb	2.2	0.8	1.0	2.1	1.0	0.7	1.2	4.3	0.3	8.8	8.3
Lu	0.29	0.12	0.15	0.31	0.16	0.11	0.19	0.61	0.05	1.29	1.17
Cr	15	36	31	10	9	7	7	120	19	7.5	120
Ni	27	11	15	36	4	1	1	290	3	14	380
Y	29	8	8	16	7	6	24	42	3	100	76
Sr	434	112	90	138	130	140	190	65	76	30	34
Zr	300	230	160	190	290	200	270	250	200	610	260
La	42.3	51.9	25.0	21.1	23.3	34.9	28.9	47.2	9.8	62.2	13.0
Ce	105.0	98.0	49.8	39.9	51.4	74.7	61.2	145.0	25.4	131.0	43.4
Pr	13.0	11.0	6.2	4.9	6.1	8.5	7.5	15.0	3.2		7.6
Nd	49.1	38.9	22.7	17.9	22.9	28.8	27.8	62.8	12.5	63.0	40.8
Sm	9.9	6.9	5.0	3.5	3.5	3.9	4.7	17.2	2.4	12.5	18.6
Eu	1.9	1.2	1.0	0.7	0.9	0.9	1.4	3.5	0.6	3.9	4.1
Gd	8.9	5.7	3.9	3.0	3.1	3.2	4.2	14.7	1.9		16.7
Tb	1.2	0.6	0.5	0.4	0.4	0.4	0.5	2.1	0.2	2.3	3

* Major element oxides expressed in wt %. All others in ppm.

Rare earth element (REE) data are shown as chondrite normalized plots for six Osmundsberg K-bentonites in Figure 11. All samples have negatively sloping curves with an overall enrichment of light rare earth elements (LREE) of approximately 100 times chondritic, and of heavy rare earth elements (HREE) a factor of 10. Both features are characteristic of calc-alkaline magmas erupted in subduction-related volcanic arc environments (Taylor & McLennan, 1988; McVey & Huff, 1995). The presence of a very slightly negative Eu anomaly suggests incomplete crystallization of plagioclase and a bulk composition that is more intermediate in composition than younger Silurian K-bentonites (Huff, Morgan & Rundle, 1997). Wenlock and Ludlow beds show LREE enrichment approximately 100–300 times chondritic and a moderate to pronounced negative Eu anomaly, indicating earlier crystallization of plagioclase. Eu/Eu* is a measure of Eu content relative to other REE such that Eu/Eu* > 1 corresponds to a positive anomaly and Eu/Eu* < 1 corresponds to a negative anomaly and indicates depletion of Eu. Mean Eu/Eu* values for 16 samples of the Osmundsberg K-bentonite are 0.83 with a standard deviation of 0.15. These features are characteristic of more highly evolved peralkaline magmas (Jakes & White, 1972) and resemble previously reported Cambrian, Ordovician and Silurian K-bentonite compositions (Roberts & Merriman, 1990; Huff *et al.* 1993). The lack of correspondingly depleted HREE indicates the fractionation of phases such as garnet and clinopyroxene did not

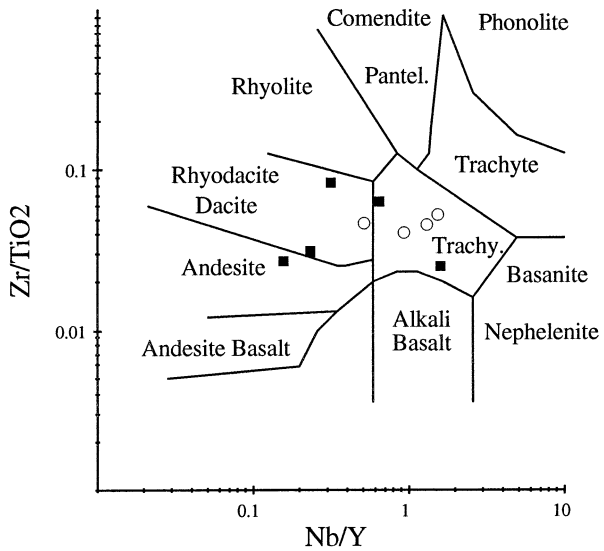

Figure 9. Plot of whole rock Zr/TiO_2 against Nb/Y after Winchester & Floyd (1977) for Osmundsberg (open circles) and coeval beds (closed squares). Samples range from subalkaline to alkaline and indicate a felsic nature for the parental magma.

Table 2. Composition* of pristine melt inclusions (n = 14) from quartz in the Osmundsberg K-bentonite

Oxide	Mean	Standard deviation	Anhydrous
SiO_2	73.08	1.36	77.71
TiO_2	0.07	0.04	0.07
Al_2O_3	12.18	0.37	12.95
FeO (total Fe)	0.68	0.27	0.72
MnO	0.03	0.03	0.03
MgO	0.05	0.03	0.05
CaO	0.97	0.16	1.03
Na_2O	3.00	0.36	3.19
K_2O	3.89	0.82	4.13
SO_3	0.01	0.02	0.01
F	0.02	0.05	0.01
Cl	0.08	0.03	0.08
Total	94.03	1.06	100

* Determined by electron microprobe and expressed in weight percent oxide. See Huff *et al.* (1996) for instrument operation conditions.

play a major role in the evolution of these calc-alkaline magmas.

Geochemical information concerning the tectonomagmatic origin of K-bentonites is provided by several widely referenced discrimination plots. In Figure 12 a plot of the immobile elements Nb against Y shows that the majority of Osmundsberg K-bentonites lie in the field of volcanic arc and syn-collision granites as defined by Pearce, Harris & Tindle (1984), suggesting that some upper mantle components still dominate the magma chemistry. It may well be that the source volcanic rocks represent the mixing of two or more primary granites in various proportions, as documented by Hildreth, Halliday & Christiansen (1991) for the Yellowstone Plateau volcanic field. Granites and alkali granites are the petrogenetic equivalents of silicic K-bentonites and these data

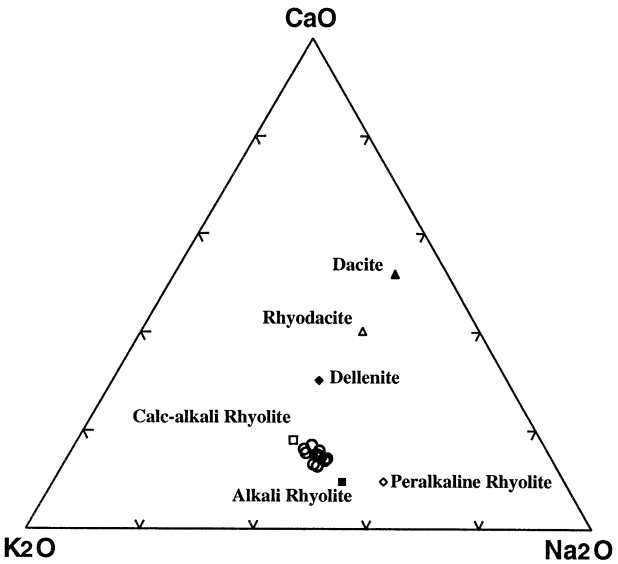

Figure 10. K_2O–CaO–Na_2O ternary plot of glass inclusions (open circles) in quartz phenocrysts from the Osmundsberg K-bentonite as compared with average acidic volcanic rocks (data from Nockolds, 1954), showing a parental magma composition between calc-alkali and alkali rhyolites.

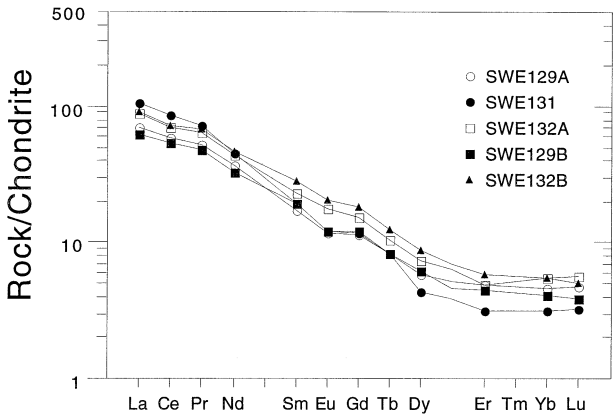

Figure 11. Chondrite normalized REE patterns for six Osmundsberg K-bentonite samples. All are enriched in LREE.

argue for a volcanic origin in a collision margin setting related to subduction. A similar conclusion was reached by Huff *et al.* (1993) for late Ordovician K-bentonites in the UK, and the Silurian beds may be seen as a continuation of that situation.

5. Chemical fingerprinting

Stratigraphic correlation of Quaternary and Holocene tephra layers frequently benefits from the use of layer-specific chemical and mineralogical information as identifying fingerprints. Explosive, rapidly-deposited ashes are particularly useful for chemostratigraphic methods because they tend to be uniform in composition throughout the entire layer, in contrast to the cumulative pyroclastic deposits of ongoing eruptions which may display bulk compositional changes reflecting long-term magmatic evolutionary processes. The widespread distribution and fine-grained nature of the Osmundsberg K-bentonite indicates that it resulted from a short-lived, large-scale explosive eruption and, like some similar Ordovician ash beds, may be the result of a co-ignimbrite eruption (Huff *et al.* 1996). Previous studies have shown that Palaeozoic K-bentonites can be correlated on a regional scale by using whole rock chemical fingerprinting based on trace element ratios, despite the alteration of primary glass. Kolata *et al.* (1987) and Huff & Kolata (1989), for example, used between-bed differences in certain trace elements to distinguish between, and correlate, the Middle Ordovician Deicke and Millbrig K-bentonites in the eastern Midcontinent of North America. This method, which is based on the relative frequency of mainly immobile trace elements in each ash bed, has proved to be a powerful tool for distinguishing between ashes from different eruptions, particularly when used in conjunction with biostratigraphic and lithostratigraphic information. Other chemostratigraphic methods which have been used successfully on Palaeozoic K-bentonites include the compositional similarity of glass melt inclusions (Delano *et al.* 1994) and the composition of primary phenocrysts (Batchelor & Jeppsson, 1994; Yost *et al.* 1994; Haynes, Melson & Kunk, 1995).

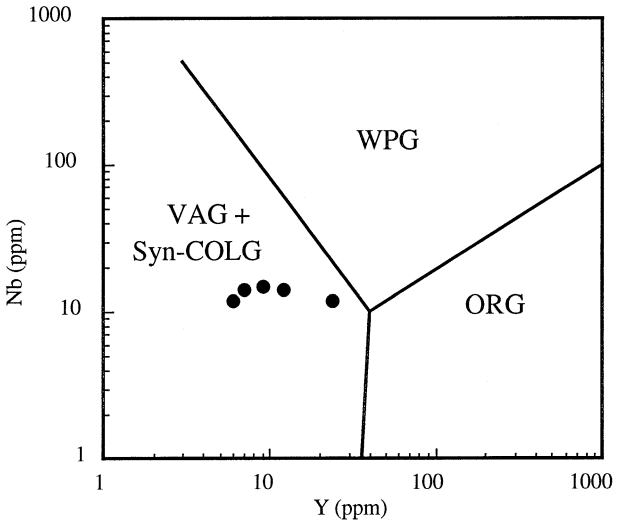

Figure 12. Plot of five Osmundsberg samples on a granite discrimination diagram after the method of Pearce, Harris & Tindle (1984). All samples indicate affinities with a volcanic to syn-collision tectonomagmatic setting. WPG – within plate granites; ORG – ocean ridge granites; VAG + Syn COLG – volcanic arc granites plus syn-collision granites.

For this study the selection of elements for chemical fingerprinting was based on discriminant function analysis of whole-rock data from stratigraphically well-constrained samples. Immobile trace elements were ranked by analysis of variance, then entered in a step-wise fashion into the discriminant model using the statistical package SPSS (SPSS, 1990). The ability of individual elements to discriminate between K-bentonite beds is enhanced when they are grouped in a hierarchical array. The linear combination of grouped variables maximizes the separation between beds in discriminant space, and the computed discriminant functions can be used to construct a discrimination diagram (Fig. 13) for identifying and correlating samples of unassigned stratigraphic position.

Table 3 Discriminant analysis summary table

Element	Wilks' Lambda
Nb	0.174
Th	0.08
Ti	0.027
Y	0.017
Sm/Nd	0.009

Silurian beds that are known to be slightly different in age from the Osmundsberg were selected to provide a basis for chemical comparison. These included a series of six Lower Silurian (Llandovery) K-bentonites from Arisaig, Nova Scotia and a group of four Wenlock K-bentonites from Estonia (Bergström, Huff & Kolata, 1992). Twelve samples of the Osmundsberg bed from the type section and surrounding area were entered as the control group, and the null hypothesis was that the between-

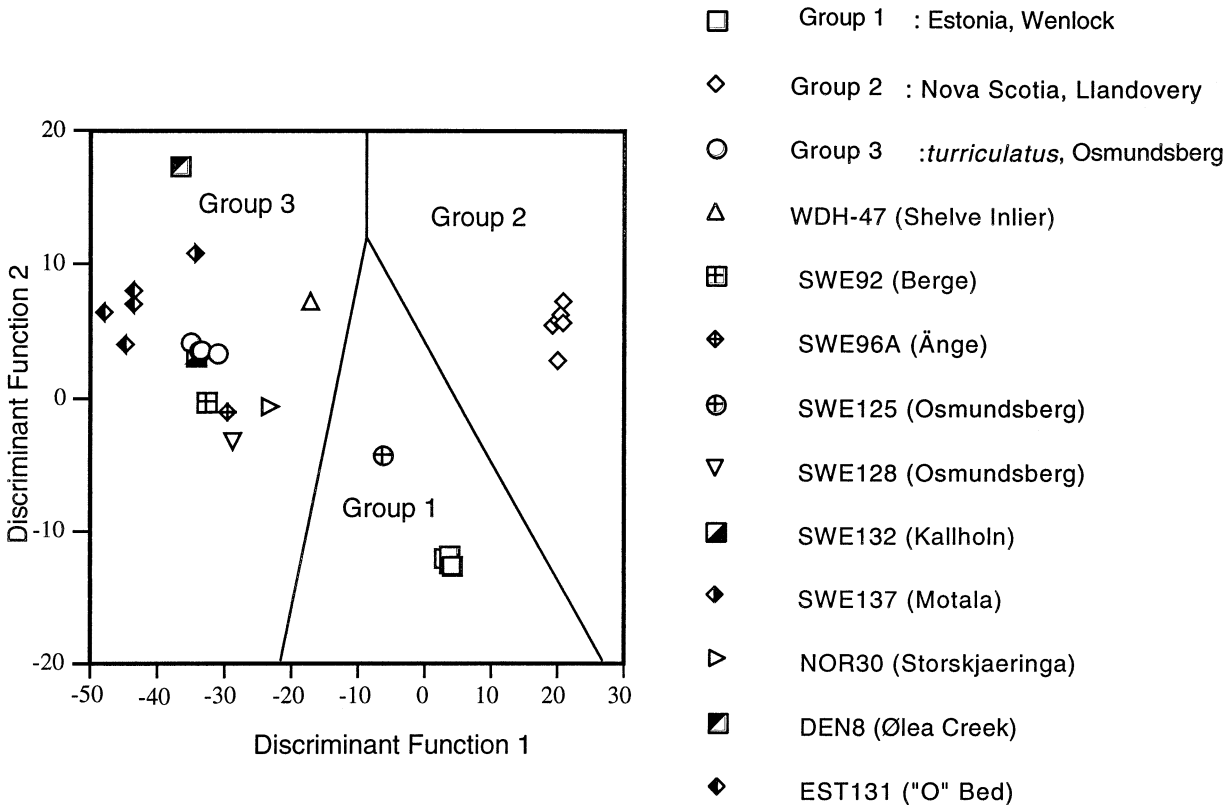

Figure 13. Territorial plot of the first and second discriminant function scores for ten coeval beds. The regions are defined by discriminant function analysis of three groups of samples representing the Osmundsberg bed, a Llandovery group from Nova Scotia, and a Wenlockian group from Estonia.

group variation in immobile element chemistry was less than the within-group variation. Twenty elements and element ratios were used in the discriminant analysis and, of these, five were found to provide maximum separation of the sample groups at the 95 % confidence level. These five are listed in Table 3 along with the corresponding values for Wilks' Lambda, an inverse measure of the ability of each element to discriminate between the three groups. Thus, Nb alone is able to explain all but 17.4 % of the variance between sample groups. When Th is added the number drops to 8.0 %. After Sm/Nd is entered, less than 1 % of the between-group variance is unexplained. These elements were also found to be effective in chemical fingerprinting of the Millbrig in North America (Kolata, Frost & Huff, 1987). Eight samples from beds which we believe to be the same as the Osmundsberg were then entered as unknowns and their discriminant scores computed. These samples represent a wide geographic distribution, but all occur as a prominent K-bentonite in the *turriculatus* Zone in Estonia, Denmark, Sweden and Norway. We also included a previously unmeasured sample from the type section as a further test of the reproducibility of the discriminant plot. As can be seen in Figure 13, all have discriminant scores that fall within the Osmundsberg region of the diagram and are thus found to be chemically more like the Osmundsberg than the other two test groups. We anticipate that further studies of melt inclusions and phenocryst chemistry should provide even more precise chemical stratigraphic parameters.

Previous work by McVey & Huff (1995) showed that population studies of primary phenocrysts can provide additional criteria for stratigraphic correlation of K-bentonites. Crystal content might well be expected to vary with distance from the source vent in volcanic plumes as a result of selective fallout near the source. However, short-range and intermediate-range correlations based on crystal content are feasible and can add further weight to correlations based on geochemical data. In Figure 14 we show the results of preliminary studies of mineralogical ratios between the type Osmundsberg bed and its nearest correlative at Kallholn, some 20 km distant. Biotite and quartz are by far the most abundant non-clay phases present, and this suggests that they may also constitute an additional physical parameter for stratigraphic usage. Within the Osmundsberg bed the quartz/biotite ratio varies indicating a non-homogeneous distribution pattern. Internal zonation of minerals in Ordovician K-bentonites has been previously noted (Haynes, 1994) and may reflect multiple ash falls closely spaced in time.

6. Discussion and conclusions

The Osmundsberg K-bentonite ranks as one of the largest fallout silicic ash beds in the lower Phanerozoic. Rare earth and other trace element data along with compositional data from melt inclusions indicate the parental magma was highly felsic in nature and most likely related to subduction. Its thickness and known pattern of distribution are of the same scale as the large Ordovician K-bentonites known from both North America and Europe. Beds of approximately the same age are known in the central Appalachian mountains of North America, but it is as yet unclear whether any of them can be correlated with the Osmundsberg. Work in progress is aimed at resolving that question. Regardless of these long-range correlations, it is clear that the Osmundsberg and associated Llandoverian K-bentonites record an interval of very large-scale explosive eruptions of silicic magma chambers. Previous studies of such phenomena (Huff *et al.* 1996) concluded the fallout ash beds were the by-product of co-ignimbrite dominated events that were sourced in plate margin caldera collapses, most likely related to active subduction of the Iapetus margin.

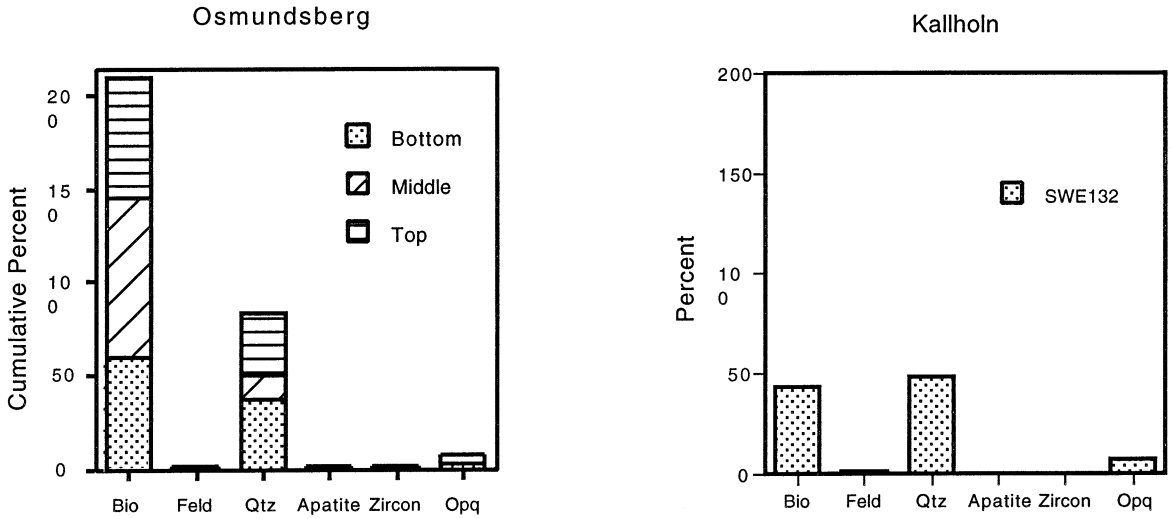

Figure 14. Results of preliminary studies of mineralogical ratios between the type Osmundsberg bed and its nearest correlative at Kallholn, some 20 km distant. Biotite and quartz are by far the most abundant non-clay phases present and this suggests that they may also constitute an additional physical parameter for stratigraphic usage.

The mid-Silurian oblique collision between Laurentia and Baltica (Torsvik *et al.* 1995) culminated a series of tectonic events which included the closure of the Tornquist Sea and the Scandian orogeny in western Norway. Both palaeomagnetic and biogeographic data used to construct palaeogeographic maps for the late Ordovician–early Silurian (Torsvik *et al.* 1996; Bergström *et al.* 1998, this issue) indicate the presence of an active southwestward dipping subduction zone along the Avalonian margin beginning in mid-Ordovician times and continuing nearly through to the time of closure of the Tornquist Sea. Continued subduction along the northern margin of the Iapetus suture is evidenced by the products of subalkaline volcanism in southwestern Ireland (Sloan & Bennett, 1990) and by structural evidence pointing to the collision between Avalonia and Laurentia (Pickering, Bassett & Siveter, 1988; Keppie, 1993). Both settings offer the potential for volcanism consistent with the composition and distribution pattern of the Osmundsberg K-bentonite. While a definitive eruptive centre has yet to be located, preliminary thickness map data suggest it lay to what is now the west of Baltoscandia (Fig. 1), and thus may have been related to late-stage closure and subduction of oceanic crust along the northwestern margin of Iapetus. The close proximity of regions known to have received Osmundsberg ash favour a Laurentian margin source, although the possibility of a still unknown active margin elsewhere, such as the southern margin of the eastern Avalonia microcontinent (Soper, 1986), cannot be dismissed. Baltica was undergoing counter-clockwise rotational movement during this interval, which introduced a significant strike-slip component to converging plate margins which makes precise tectonic reconstruction difficult. It does seem clear, however, that south-central Sweden and the surrounding Baltoscandic terrane was not far removed from a major source of subduction-related explosive volcanism.

Acknowledgements. This work was supported in part by NSF grants EAR-9204893, EAR-9004559, EAR-9205981 and EAR-9005333. We are grateful to David Bruton, Dimitri Kaljo, Heikki Bauert, Lars Karis and Bernard Anderson for advice and assistance in the field. Jan Bergström kindly arranged shipping of the Baltic samples.

References

ALTANER, S. P., HOWER, J., WHITNEY, G. & ARONSON, J. L. 1984. Model for K-bentonite formation: Evidence from zoned K-bentonites in the disturbed belt, Montana. *Geology* **12**, 412–15.

ANWILLER, D. N. 1993. Illite/smectite formation and potassium mass transfer during burial diagenesis of mudrocks: A study from the Texas Gulf Coast Paleocene–Eocene. *Journal of Sedimentary Petrology* **63**, 501–12.

BANFIELD, J. F. & EGGLETON, R. A. 1988. Transmission electron microscope study of biotite weathering. *Clays and Clay Minerals* **36**, 47–60.

BATCHELOR, R. A. & JEPPSSON, L. 1994. Late Llandovery bentonites from Gotland, Sweden, as chemostratigraphic markers. *Journal of the Geological Society* **151**, 741–6.

BATCHELOR, R. A. & WEIR, J. A. 1988. Metabentonite geochemistry: magmatic cycles and graptolite extinctions at Dob's Linn, southern Scotland. *Transactions of the Royal Society of Edinburgh: Earth Sciences* **79**, 19–41.

BERGSTRÖM, S. M., HUFF, W. D. & KOLATA, D. R. 1992. Silurian K-bentonites in the Iapetus Region: A preliminary event-stratigraphic and tectonomagmatic assessment. *Geologiska Föreningens I Stockholm Förhandlingar* **114**, 327–34.

BERGSTRÖM, S. M., HUFF, W. D. & KOLATA, D. R. 1998. The Lower Silurian Osmundsberg K-bentonite. Part I: stratigraphic position, distribution, and palaeogeographic significance. *Geological Magazine* **135**, 1–13.

BERGSTRÖM, S. M., HUFF, W. D., KOLATA, D. R. & KALJO, D. 1993. The Osmundsberg K-bentonite: a widespread volcanic ash bed in the Upper Llandoverian (Lower Silurian) of northwestern Europe. *Geological Society of America Abstracts with Programs* **25**, 75–6.

BETHKE, C. M., VERGO, N. & ALTANER, S. P. 1986. Pathways of smectite illitization. *Clays and Clay Minerals* **34**, 125–35.

BRUSEWITZ, A. M. 1988. Asymmetric zonation of a thick Ordovician K-bentonite bed at Kinnekulle, Sweden. *Clays and Clay Minerals* **36**, 349–53.

DELANO, J. W., TICE, S. J., MITCHELL, C. E. & GOLDMAN, D. 1994. Rhyolitic glass in Ordovician K-bentonites: A new stratigraphic tool. *Geology* **22**, 115–18.

HAYNES, J. T. 1994. The Ordovician Deicke and Millbrig K-bentonite beds of the Cincinnati Arch and the southern Valley and Ridge Province. *Geological Society of America Special Paper* **290**, 1–80.

HAYNES, J. T., MELSON, W. G. & KUNK, M. J. 1995. Composition of biotite phenocrysts in Ordovician tephras casts doubt on the proposed trans-Atlantic correlation of the Millbrig K-bentonite (United States) and the Kinnekulle K-bentonite (Sweden). *Geology* **23**, 847–50.

HILDRETH, W., HALLIDAY, A. N. & CHRISTIANSEN, R. L. 1991. Isotopic and chemical evidence concerning the genesis and contamination of basaltic and rhyolitic magma beneath the Yellow Plateau volcanic field. *Journal of Petrology* **32**, 63–138.

HUFF, W. D. 1997. Silurian K-bentonites of Podolia, Ukraine. *The 11th International Clay Conference Program with Abstracts, Ottawa*, 38.

HUFF, W. D., ANDERSON, T. B., RUNDLE, C. C. & ODIN, G. S. 1991. Chemostratigraphy, K–Ar ages and illitization of Silurian K-bentonites from the central belt of the Southern Uplands–Down–Longford terrane, British Isles. *Journal of the Geological Society, London* **148**, 861–8.

HUFF, W. D. & KOLATA, D. R. 1989. Correlation of K-bentonite beds by chemical fingerprinting using multivariate statistics. In *Quantitative Dynamic Stratigraphy* (ed. T. A. Cross), pp. 567–77. Englewood Cliffs, New Jersey, USA: Prentice-Hall.

HUFF, W. D. & KOLATA, D. R. 1990. Correlation of the Ordovician Deicke and Millbrig K-bentonites between the Mississippi Valley and the southern Appalachians. *American Association of Petroleum Geologists Bulletin* **74**, 1736–47.

HUFF, W. D., KOLATA, D. R., BERGSTRÖM, S. M. & ZHANG, Y.-S. 1996. Large-magnitude Middle Ordovician volcanic ash falls in North America and Europe: dimensions, emplacement and post-emplacement characteristics. *Journal of Volcanology and Geothermal Research* **73**, 285–301.

HUFF, W. D., MERRIMAN, R. J., MORGAN, D. J. & ROBERTS, B. 1993. Distribution and tectonic setting of Ordovician K-bentonites in the United Kingdom. *Geological Magazine* **130**, 93–100.

HUFF, W. D., MORGAN, D. J. & RUNDLE, C. C. 1997. *Silurian K-bentonites of the Welsh Borderlands: Geochemistry, mineralogy and K-Ar ages of illitization.* British Geological Survey, Report WG/96/45, 25 pp.

IZETT, G. A. 1981. Volcanic ash beds: Recorders of Upper Cenozoic silicic pyroclastic volcanism in the western United States. *Journal of Geophysical Research* **86**, 10200–22.

JAKES, P. & WHITE, A. J. R. 1972. Major and trace element abundances in volcanic rocks of orogenic areas. *Geological Society of America Bulletin* **83**, 29–40.

JIANG, W.-T. & PEACOR, D. R. 1994. Prograde transitions of corrensite and chlorite in low-grade pelitic rocks from the Gaspé Peninsula, Quebec. *Clays and Clay Minerals* **42**, 497–517.

KEPPIE, J. D. 1993. Synthesis of Palaeozoic deformational events and terrane accretion in the Canadian Appalachians. *Geologische Rundschau* **82**, 381–431.

KOLATA, D. R., FROST, J. K. & HUFF, W. D. 1987. Chemical correlation of K-bentonites in the Middle Ordovician Decorah Subgroup, upper Mississippi Valley. *Geology* **15**, 208–11.

KREKELER, M. P. S. & HUFF, W. D. 1993. Occurrence of corrensite and ordered (R3) illite/smectite (I/S) in a VLGM Middle Ordovician K-bentonite from the Hamburg Klippe, central Pennsylvania. *Geological Society of America Abstracts with Programs* **25**, 30.

MCKERROW, W. S., DEWEY, J. F. & SCOTESE, C. R. 1991. The Ordovician and Silurian development of the Iapetus Ocean. *Special Papers in Palaeontology* **44**, 165–78.

MCVEY, D. E. & HUFF, W. D. 1995. Southern and central Appalachian stratigraphy interpreted with the use of the Middle Ordovician Deicke and Millbrig K-bentonite beds. In *Ordovician Odyssey: Short papers for the Seventh International Symposium on the Ordovician System* (eds J. D. Cooper, M. L. Droser and S. C. Finney), pp. 351–3. The Pacific Section Society for Sedimentary Geology Book 77.

MERRIMAN, R. J. & ROBERTS, B. 1990. Metabentonites in the Moffat Shale Group, Southern Uplands of Scotland: Geochemical evidence of ensialic marginal basin volcanism. *Geological Magazine* **127**, 259–71.

MOORE, D. M. & REYNOLDS, R. C. JR. 1989. *X-ray diffraction and the identification and analysis of clay minerals*. Oxford University Press, 332 pp.

NOCKOLDS, S. R. 1954. Average chemical compositions of some igneous rocks. *Geological Society of America Bulletin* **65**, 1007–32.

PEARCE, J. A., HARRIS, N. B. W. & TINDLE, A. G. 1984. Trace element discrimination diagrams for the tectonic interpretation of granitic rocks. *Journal of Petrology* **25**, 956–83.

PICKERING, K. T., BASSETT, M. G. & SIVETER, D. J. 1988. Late Ordovician–Early Silurian destruction of the Iapetus Ocean: Newfoundland, British Isles and Scandinavia. *Transactions of the Royal Society of Edinburgh: Earth Sciences* **79**, 361–82.

REYNOLDS, R. C. JR. 1985. *NEWMOD: A computer program for the calculation of one-dimensional diffraction patterns of mixed-layer clays*. R. C. Reynolds, 8 Brook Rd., Hanover, New Hampshire, USA.

ROBERTS, B. & MERRIMAN, R. J. 1990. Cambrian and Ordovician metabentonites and their relevance to the origins of associated mudrocks in the northern sector of the Lower Palaeozoic Welsh marginal basin. *Geological Magazine* **127**, 31–43.

SLOAN, R. J. & BENNETT, M. C. 1990. Geochemical character of Silurian volcanism in SW Ireland. *Journal of the Geological Society, London* **147**, 1051–60.

SOPER, N. J. 1986. The Newer Granite problem: a geotectonic perspective. *Geological Magazine* **123**, 227–36.

SPSS. 1990. *SPSS 6.1 Base System User's Guide, Part 1*. SPSS Inc., 444 N. Michigan Ave., Chicago, Illinois, USA, 250 pp.

TAYLOR, S. R. & MCLENNAN, S. M. 1988. The significance of the rare earths in geochemistry and cosmochemistry. In *Handbook on the physics and chemistry of rare earths* (eds K. A. Gschneider and L. Eyring), pp. 485–578. New York: Elsevier.

TEALE, C. T. & SPEARS, D. A. 1986. The mineralogy and origin of some Silurian bentonites, Welsh Borderland, U.K. *Sedimentology* **33**, 757–65.

TORSVIK, T. H., SMETHURST, M. A., MEERT, J. G., VAN DER VOO, R., MCKERROW, W. S., BRASIER, M. D., STURT, B. A. & WALDERHAUG, H. J. 1996. Continental break-up and collision in the Neoproterozoic and Palaeozoic – A tale of Baltica and Laurentia. *Earth-Science Reviews* **40**, 229–58.

TORSVIK, T. H., TAIT, J., MORALEV, V. M., MCKERROW, W. S., STURT, B. A. & ROBERTS, D. 1995. Ordovician palaeogeography of Siberia and adjacent continents. *Journal of the Geological Society, London* **152**, 279–87.

WINCHESTER, J. A. & FLOYD, P. A. 1977. Geochemical discrimination of different magma series and their differentiation products using immobile elements. *Chemical Geology* **20**, 325–43.

YOST, D. A., HUFF, W. D., BERGSTRÖM, S. M. & KOLATA, D. R. 1994. Use of mineralogical and geochemical data for high resolution stratigraphic correlation of a Middle Ordovician K-bentonite. *Geological Society of America Abstracts with Programs* **26**, 81.